

Quantum Monte Carlo Study of Weakly Coupled Spin Ladders

Y. J. Kim

*Division of Engineering and Applied Sciences, Harvard University, Cambridge, Massachusetts 02138
and Center for Materials Science and Engineering, Massachusetts Institute of Technology, Cambridge, Massachusetts 02139*

R. J. Birgeneau, M. A. Kastner, and Y. S. Lee

Department of Physics and Center for Materials Science and Engineering, Massachusetts Institute of Technology, Cambridge, Massachusetts 02139

Y. Endoh

Department of Physics, Tohoku University, Sendai 980-8578, Japan

G. Shirane

Department of Physics, Brookhaven National Laboratory, Upton, New York 11973

K. Yamada

*Department of Physics, Kyoto University, Gokasho, Uji 610-0011, Japan
(October 25, 2019)*

We report a quantum Monte Carlo study of the thermodynamic properties of arrays of spin ladders with various widths (n), coupled via a weak inter-ladder exchange coupling αJ , where J is the intra-ladder coupling both along and between the chains. This coupled ladder system serves as a simplified model for the magnetism of presumed ordered spin and charge stripes in the two-dimensional CuO_2 planes of hole-doped copper oxides. Our results for $n = 3$ with weak inter-ladder coupling $\alpha = 0.05$, estimated from the $t - t' - t'' - J$ model, show good agreement with the ordering temperature of the recently observed spin density wave condensation in $\text{La}_2\text{CuO}_{4+y}$. We show that there exists a quantum critical point at $\alpha_c \simeq 0.07$ for $n = 4$, and determine the phase diagram. Our data at this quantum critical point agree quantitatively with the universal scaling predicted by the quantum nonlinear σ model. We also report results on random mixtures of $n = 2$ and $n = 3$ ladders, which correspond to the doping region near but above $1/8$. Our study on the magnetic static structure factor reveals a saturation of the incommensurability of the spin correlations around $1/8$, while the incommensurability of the charge stripes grows linearly with hole concentration. The implications of this result for the interpretation of neutron scattering experiments on the dynamic spin fluctuations in $\text{La}_{2-x}\text{Sr}_x\text{CuO}_4$ are discussed.

I. INTRODUCTION

One of the most surprising early observations in the field of high temperature superconductivity is that the onset of superconductivity as a function of hole concentration coincides with a commensurate-incommensurate transition in the low-energy dynamical spin fluctuations.¹ These incommensurate spin fluctuations have been studied extensively over the past decade.² We note especially the recent detailed quantitative study by Yamada *et al.*³ A variety of theoretical explanations of the spin incommensurability have been offered, varying from nesting of the Fermi surface in a nearly free electron model⁴⁻⁶ to microscopic phase separation of the holes in a doped-Mott insulator model for the copper oxides.⁷⁻⁹ Specifically, in the latter model under certain circumstances the holes could organize themselves into *stripes* with the charged stripes acting as antiphase domain walls for the intervening antiferromagnetic regions. The latter correspond to spin ladders which have been recently studied quite extensively in a different context.^{10,11} None of the experiments on the spin dynamics has been able to select

unambiguously between these various theoretical models.

However, in the past two years, the experimental situation has changed significantly. First, rather dramatic elastic magnetic scattering effects have been observed¹² at low temperatures in samples of $\text{La}_{1.6-x}\text{Nd}_{0.4}\text{Sr}_x\text{CuO}_4$ with $x=0.12, 0.15, \text{ and } 0.20$. These materials are all superconductors with onset T_c 's of $\simeq 4K, 11K$ and $15K$, respectively. In each case, Tranquada and coworkers observe elastic incommensurate magnetic peaks with onset temperatures of $\simeq 50K, 46K$ and $15K$, respectively. Recent work¹³ has shown that in the $x=0.12$ sample the correlation length reaches its maximum value below $\sim 30K$. The incommensurabilities are essentially identical to those of the corresponding dynamical fluctuations in samples of $\text{La}_{2-x}\text{Sr}_x\text{CuO}_4$ with the same x . In their study of the spin dynamics in $\text{La}_{2-x}\text{Sr}_x\text{CuO}_4$, Yamada *et al.* observe that the momentum space width of the low-energy spin fluctuations is a minimum for hole concentrations near $1/8$. Further, at these hole concentrations the spin fluctuations extend down to very low energies even in the superconducting state. This is in contrast to the situation in samples with hole concentrations at

and above the optimal doping level, $x \simeq 0.15$, where a well-defined spin gap is observed in the superconducting state. This has led Suzuki *et al.*¹⁴ and more recently, Kimura *et al.*¹⁵ to search for elastic magnetic scattering effects in $\text{La}_{1.88}\text{Sr}_{0.12}\text{CuO}_4$. Remarkably, they observe a spin density wave transition at $T_m \simeq 31\text{K}$ which coincides to within the errors with the onset temperature for superconductivity in this sample; the incommensurability is $\epsilon = 0.12$ which equals the Sr-doping, x . Kimura and coworkers also observe magnetic order in a sample of $\text{La}_{1.90}\text{Sr}_{0.10}\text{CuO}_4$ ($T_c = 31\text{K}$) with incommensurability $\epsilon = 0.105$ below $T_m \simeq 15\text{K}$.

Most recently, Lee and coworkers¹⁶ have searched for spin density wave order in a sample of La_2CuO_4 doped with oxygen, that is, $\text{La}_2\text{CuO}_{4+y}$, which has a superconducting T_c (onset) of 42K and is predominantly stage-4. They indeed find a transition to long-range incommensurate magnetic order at $T_m \simeq 42\text{K}$ with typical Bardeen–Cooper–Schrieffer (BCS) mean field behavior of the order parameter below T_m . Importantly, they find that both the spin ordering direction and the three dimensional stacking arrangement coincide with those in pure La_2CuO_4 . The magnetic structure can be modeled quite well with $n = 3$ stripes of the La_2CuO_4 in-plane structure separated by $n = 1$ non-magnetic antiphase domain walls; this gives an incommensurability $\epsilon = 0.125$, close to the measured value. The measured long-range ordered moment is $\sim 0.15\mu_B$ and the inter-layer magnetic correlation length is ~ 3 CuO_2 layers.

In our view, these observations, including especially this recent work on $\text{La}_2\text{CuO}_{4+y}$, give credence to stripe models for the microscopic magnetic structure. The recent observation¹⁷ of similar incommensurabilities in the spin dynamics of underdoped $\text{YBa}_2\text{Cu}_3\text{O}_{6.6}$ strengthens this argument. Of course, a great deal of work remains to be done to explain all of the experimental observations, especially the electronic properties in the normal and superconducting states. Kivelson *et al.*¹⁸ consider the electronic degrees of freedom within the charge stripes and characterize these phases as electronic liquid crystals. Although the charge and spin degrees of freedom of the charged stripes themselves are clearly essential to the physics, it is nevertheless important as a first step to develop a deeper understanding of the simpler problem of the magnetism of idealized insulating stripe arrays as a function of stripe width or, equivalently, hole concentration. Accordingly, we adopt a naive model, in which for hole concentrations between ~ 0.05 and 0.15 there is approximately one hole per two coppers^{12,19} along site-centered charge stripes running along the tetragonal $\text{Cu-O-Cu-O}\dots$ axes with the holes confined to single chains. We assume further that the charge stripes are effectively non-magnetic and that the magnetic coupling across the stripes is, to first order, determined by the third-nearest-neighbor coupling within the CuO_2 plane. This is believed to be antiferromagnetic and to be about 5% of the nearest neighbor coupling.²⁰ We omit entirely any effects of the low energy charge and spin excitations of

the charged stripes themselves. In this greatly simplified model, one may use standard quantum Monte Carlo (QMC) techniques to determine the magnetic properties of the stripe arrays.

Our understanding of two-dimensional quantum magnetism has grown enormously since the discovery of high temperature superconductivity. Theoretical efforts to understand the underlying antiferromagnetism in the parent compounds as well as experimental efforts to synthesize and study new cuprate materials have both contributed significantly. In particular, the two-dimensional quantum Heisenberg antiferromagnet (2DQHA) has been studied extensively, since the pioneering work by Chakravarty, Halperin, and Nelson.²¹ They have mapped the long-wavelength, low-temperature behavior of the 2DQHA to a quantum nonlinear σ model (QNL σ M) in (2+1) dimensions and have obtained a phase diagram with three regimes; quantum disordered (QD), quantum critical (QC), and renormalized classical (RC). They have argued that the 2DQHA on the square lattice for $S \geq 1/2$ with nearest neighbor interactions is in the RC regime, and consequently has a correlation length diverging exponentially in $1/T$ as temperature is lowered to $T = 0$, implying the existence of a long-range ordered ground state. The temperature dependence of the correlation length in the RC regime, which has been solved exactly to three loop order by Hasenfratz and Niedermayer (HN),²² agrees quantitatively with the results of neutron scattering experiments on both $\text{Sr}_2\text{CuO}_2\text{Cl}_2$ ²³ and La_2CuO_4 .²⁴

One-dimensional (1D) quantum magnetism has also drawn much interest in the last decade, mainly due to a conjecture made by Haldane regarding the different ground state properties between spin chains with integer and half-integer spin quantum number.²⁵ In his seminal work in 1983,²⁶ Haldane mapped the 1D Heisenberg model onto the QNL σ M and showed that the half-integer spin chain has an additional topological term, which generates gapless low-energy excitations together with algebraically decaying spin correlation functions. Integer spin chains, however, can be described by the standard QNL σ M in (1+1) dimensions, in which the ground state is disordered due to quantum fluctuations and the excitation spectrum acquires a gap – the so-called *Haldane gap*. This conjecture has been subsequently confirmed both numerically²⁷ and experimentally.²⁸ Spin ladders have been studied mostly in the same context;¹⁰ when even numbers of $S = 1/2$ chains are coupled to form a ladder (even-width), they show the same universal behavior as integer spin chains, while odd-width $S = 1/2$ ladders behave essentially like a single $S = 1/2$ chain at low temperatures and long wavelengths.

In this paper we report a detailed QMC study of ladder arrays as a function of the width of the spin ladders (n), the strength of the coupling across the non-magnetic line ($J' = \alpha J$), and temperature (T). We have carried out such calculations for $n = 4$ ladder arrays, $n = 3$ ladder arrays, and for random mixtures of $n = 3$ and $n = 2$ lad-

ders. These various arrays are illustrated in Fig. 1. In the limit of $\alpha \rightarrow 0$, the model corresponds to a set of isolated ladders, and in the limit $\alpha \rightarrow 1$ we recover the isotropic $S = 1/2$ square lattice QHA. One can easily see that a quantum critical point as a function of α should exist for non-zero α for coupled even-width ladders. Indeed, the recent study by Tworzydło *et al.*²⁹ shows that $\alpha_c \simeq 0.3$ for coupled $n = 2$ ladders. We show that arrays of $n = 4$ ladders exhibit a quantum critical point around $\alpha \simeq 0.07$. We discuss our QMC results in the context of available experimental information; we also suggest future measurements which should determine whether or not these calculations are in fact relevant to the real monolayer CuO_2 superconductors.

The format of this paper is as follows: In Sec. II we discuss our QMC techniques. Section III contains our results for weakly coupled three-leg ladders ($n = 3$). Results for weakly coupled four-leg ladders ($n = 4$) including especially the quantum critical behavior are given in Sec. IV. In Sec. V, we discuss the results for random mixtures of two-leg and three-leg ladders. We have also studied strongly coupled $n = 3$ ladders and present the results in Sec. VI. Finally, a discussion, summary, and conclusions are given in Sec. VII.

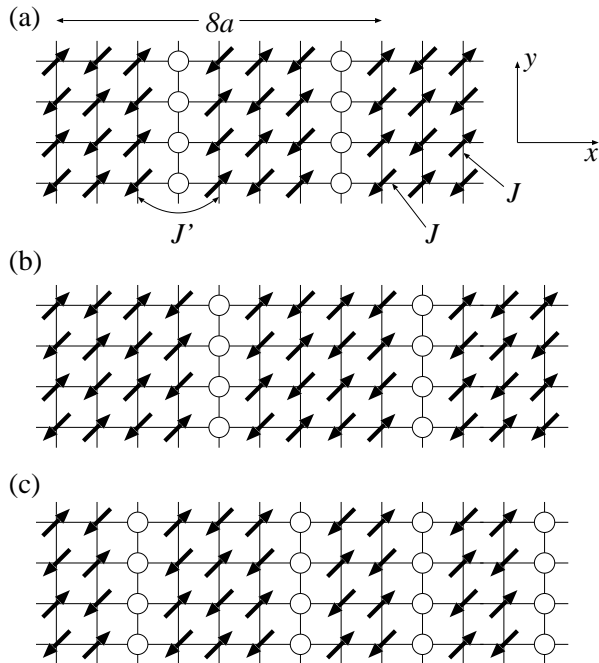


FIG. 1. Schematic diagram of the model. (a) Weakly coupled three leg ladder array with a periodicity of $8a$. J' is the inter-ladder coupling αJ . (b) Weakly coupled four leg ladder array. (c) Random mixture of two and three leg ladders.

II. QUANTUM MONTE CARLO

We have carried out quantum Monte Carlo simulations on large lattices utilizing the loop cluster algorithm.³⁰

The same algorithm previously employed to study spin ladders¹¹ and chains³¹ is used with minor modifications. We obtain the temperature dependence of the uniform susceptibility, $\chi_u(T)$, the spin-spin correlation length in the x -direction, $\xi_x(T)$, and the y -direction, $\xi_y(T)$, the staggered susceptibility, $\chi_s(T)$, and the static structure factor at the antiferromagnetic wave vector $\mathbf{Q} \equiv (\pi, \pi)$, $S_Q(T)$. The Hamiltonian for our model is based on the square lattice with a coupling J , but every n -th bond in the x -direction is replaced by a bond with exchange coupling αJ :

$$\mathcal{H} = J \left[\sum_{i,j} \mathbf{S}_{i,j} \cdot \mathbf{S}_{i,j+1} + \sum_{i \neq ln, j} \mathbf{S}_{i,j} \cdot \mathbf{S}_{i+1,j} + \alpha \sum_{i=ln, j} \mathbf{S}_{i,j} \cdot \mathbf{S}_{i+1,j} \right], \quad (1)$$

where i and j run over the x and y directions, respectively. n is the width of the ladder and l counts the ladders. We use units in which $\hbar = k_B = g\mu_B = 1$. We also set the lattice constant $a = 1$. Periodic boundary conditions are used in both directions.

One should note that, although this Hamiltonian captures the essential magnetic interactions of coupled ladders, if Eq. (1) is to describe the stripe arrays shown in Fig. 1, the lattice constant in the x -direction is $\frac{n}{n+1}$ instead of one. This affects only two quantities in our computation; $\xi_x(T)$ and $S_Q(T)$. The correction for $\xi_x(T)$ is trivial, since $\xi_x(T)$ is measured in units of the lattice constant. Unless noted otherwise, this $\frac{n}{n+1}$ correction is incorporated in the ξ_x data presented in this paper. $S_Q(T)$, however, cannot be converted in a simple manner for the stripe model. Therefore, in the following sections, $S_Q(T)$ should be understood as the structure factor at (π, π) for the model Hamiltonian, Eq. (1), rather than for the stripe model as shown in Fig. 1. The incommensurate structure factor is discussed only in Sec. V, where it is separately computed as a function of q_x , $S(q_x, \pi)$.

In order to deduce the spin-spin correlation lengths, $\xi_x(T)$ and $\xi_y(T)$, the instantaneous spin-spin correlation function, $C(x, y)$, is computed and fitted to the asymptotic form

$$C(x, 0) \sim x^{-\lambda} e^{-x/\xi_x} + (L_x - x)^{-\lambda} e^{-(L_x - x)/\xi_x} \quad (2a)$$

$$C(0, y) \sim y^{-\lambda} e^{-y/\xi_y} + (L_y - y)^{-\lambda} e^{-(L_y - y)/\xi_y}, \quad (2b)$$

which is a symmetrized 2D Ornstein-Zernike form ($\lambda = 0.5$). Only data with $x \gtrsim 3\xi_x$ and $y \gtrsim 3\xi_y$ are included in the fits to ensure that the asymptotic behavior is probed. Technically, due to the non-uniformity of the exchange couplings in the x -direction, $C(x, 0)$ can be better described by the function $\sim x^{-1/2} e^{-x/\xi_x} \sin(x/n)$ rather than Eq. (2a); however, the values for ξ_x obtained with both methods agree within the error bars.

The lengths and Trotter numbers of the simulated lattices are chosen so as to minimize any finite-size and

lattice-spacing effects. The linear sizes of the lattice, L_x and L_y , are kept at least 10 times larger than the respective correlation lengths. Spin states are updated about 2×10^4 times to reach equilibrium and then measured $\sim 5 \times 10^4$ times. For the random mixtures of $n = 2$ and $n = 3$ ladders, we generate each configuration in the following way: Beginning from the first column ($i = 1$), we assign a spin or hole for each column; the number of spin columns between the hole columns represents the width of the spin stripe. In order to make sure that the width is either two or three, we put restrictions such that a spin column must be assigned after each hole column, while a hole column must be assigned after three consecutive spin columns. The width of each ladder is determined by generating a random number r ($0 < r < 1$) and comparing r with p , where p is the ratio of the three leg ladder in the mixture. After two spin columns are assigned, the spin column is assigned only if $r < p$, otherwise the hole column is assigned and the width becomes two. For example, for an equal mixture of two and three leg ladders, $p = 0.5$. For each T and p , typically 10 to 20 different configurations are generated and averaged over. Averaging over more configurations does not alter our results.

III. WEAKLY COUPLED THREE LEG LADDERS

We present our QMC data for the $n = 3$ case, Fig. 1(a), in this section. From detailed studies of isolated ladders,¹¹ it is known that at low temperatures and long length scales three-leg ladders exhibit the same behavior as a single chain ($S = 1/2$). It is well known that any non-zero inter-ladder coupling eventually enhances the correlations across the non-magnetic stripe and drives the system towards the 2DQHA-QNL σ M RC fixed point. Thus, we expect to see qualitatively different behavior for an array of weakly coupled $n = 3$ ladders from that of isolated ladders. The correlation lengths for arrays of $n = 3$ ladders are shown in Fig. 2 as a function of inverse temperature for various inter-ladder couplings (α). Note that $\alpha = 0$ corresponds to an isolated three leg ladder; these data are taken from Ref. 11. Not surprisingly, one can see clearly $\sim \exp(1/T)$ behaviors except for $\alpha = 0$, as discussed above. In the inset of Fig. 2, we also show the ratio ξ_y/ξ_x . At low temperatures, ξ_y/ξ_x approaches the mean field prediction, $\sqrt{\alpha}$, shown here as a solid line for each α .

Our correlation length data are fitted to the crossover form given by Castro Neto and Hone,³² which interpolates between the HN result at low temperatures and $\xi \sim T^{-1}$ at high temperatures:

$$\xi = A \exp\left(\frac{2\pi\rho_s}{T}\right) \frac{1}{1 + \frac{1}{2} \frac{T}{2\pi\rho_s}}, \quad (3)$$

where ρ_s is the spin stiffness. Our fitting results are presented in Table I. We note first that the values deduced for $2\pi\rho_s$ separately from ξ_y and ξ_x are the same within

the error bars, which means that there is only one temperature scale for the low-temperature behavior of this model, despite the fact that the correlation lengths themselves are highly anisotropic.

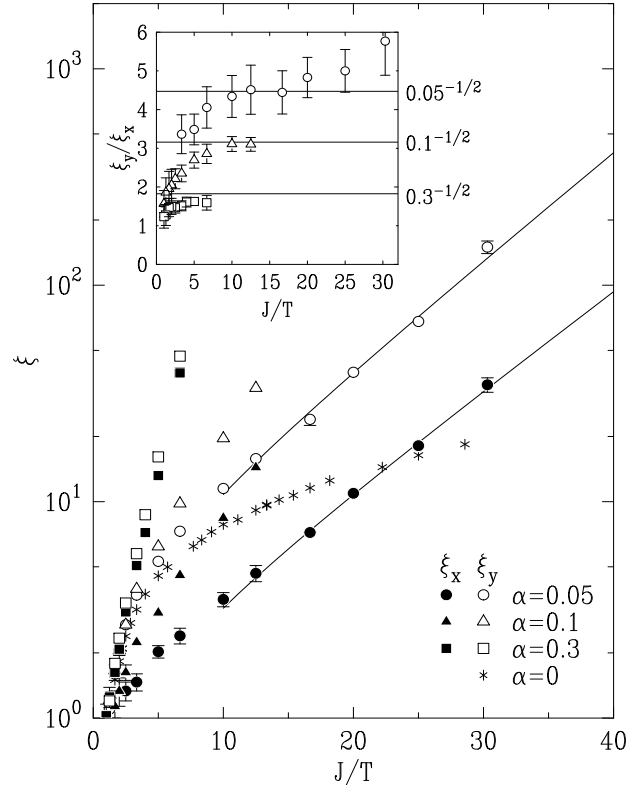


FIG. 2. Correlation lengths for arrays of $n = 3$ ladders with different inter-ladder coupling α plotted as a function of inverse temperature. Correlation lengths in the x -direction are shown as solid symbols, while those in the y -direction are shown as empty symbols. For $\alpha = 0.05$, the fitting results from Eq. (3) are also plotted. Inset: The ratio of ξ_y/ξ_x . Each solid line corresponds to the mean field value, $\sqrt{\alpha}$. The ratio is given without the $n/(n+1)$ correction discussed in Sec. II.

TABLE I. Fitting parameters for $n=3$ data to Eq. (3) without the $n/(n+1)$ correction.

α	$2\pi\rho_s/J$		A	
	ξ_x	ξ_y	ξ_x	ξ_y
0.05	0.10(1)	0.11(1)	0.26(2)	1.14(5)
0.1	0.17(2)	0.19(1)	0.52(5)	1.4(1)
0.3	0.55(2)	0.58(1)	0.83(5)	1.22(5)
1.0 ^a	1.1310(3)		0.4978(8)	

^aRef. 36

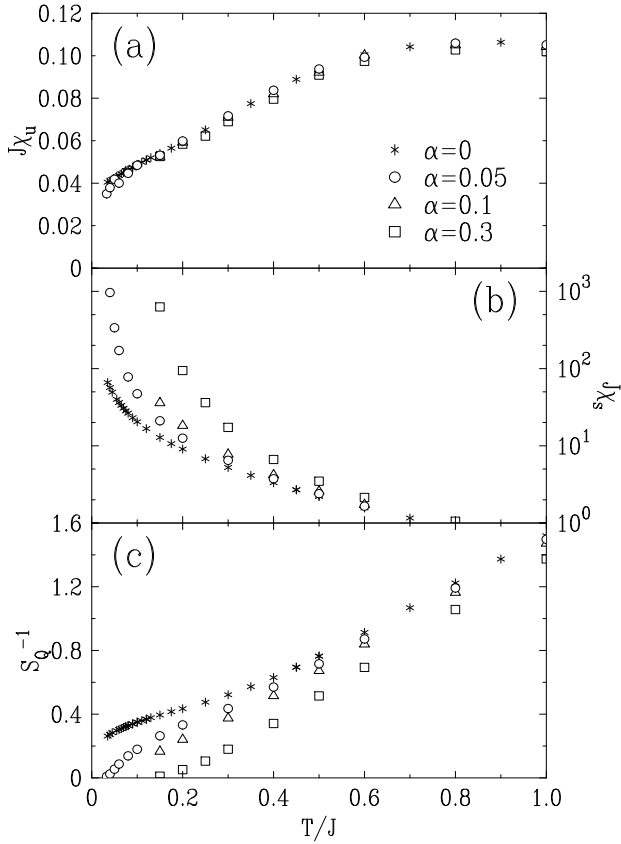


FIG. 3. Uniform susceptibility, staggered susceptibility, and inverse static structure factor peak intensity for arrays of $n = 3$ ladders with different inter-ladder couplings α .

Since the 2D Heisenberg model cannot have long-range order at any non-zero temperature, either a small anisotropy in the spin Hamiltonian or a non-zero 3D coupling is necessary to explain the Néel transition in real materials. In pure La_2CuO_4 , one can estimate the Néel transition temperature reliably as the temperature at which the correlation length squared becomes of order of the inverse of the effective anisotropy,³³ which, in the case of La_2CuO_4 , is about $\gamma_{eff} \approx 10^{-4}$. We can apply the same heuristic formula to determine the spin density wave ordering temperature, T_m , for our presumed stripe array model for doped La_2CuO_4 . For example, $\text{La}_2\text{CuO}_{4+y}$ has the same spin ordering direction and stacking scheme as in pure La_2CuO_4 except that the inter-layer order extends over only about three planes;¹⁶ thus, we take the same effective anisotropy and find the temperature satisfying $\xi_x(T_m)\xi_y(T_m) \approx \gamma_{eff}^{-1}$. In our simplified model the inter-ladder coupling is determined by the third-nearest-neighbor exchange coupling in the CuO_2 plane; from current values for t, t', t'' and J in the extended $t - J$ model²⁰ we estimate $\alpha \approx (t''/t)^2 \approx 0.05$. By extrapolating our correlation length data to lower temperature for $\alpha = 0.05$, we obtain $T_m \approx 0.029J$, or $T_m \approx 44K$ for $J = 1500K$, which agrees remarkably well with the experimental result. This precise agreement is a coincidence since $\alpha = 0.05$ is only a crude estimate and

we have assumed perfectly ordered charge stripes. We note that $\alpha = 0.1$ gives $T_m \approx 75K$. We should also note that these estimates of T_m 's are not very sensitive to the explicit value of γ_{eff} . Even if γ_{eff} changes by a factor of two, T_m remains within 10% of the value obtained here. However, T_m depends sensitively on the choice of the inter-ladder exchange coupling αJ . The low values for T_m found experimentally clearly constrain the inter-ladder coupling to rather small values (or, as discussed in Sec. VI, very large values), at least within the simplified model considered here.

In Fig. 3, Monte Carlo results for χ_u , χ_s , and the inverse of S_Q are plotted as a function of T , for different α 's. The reason S_Q^{-1} is plotted is to emphasize the effect of the inter-ladder coupling. One of the most significant results of Ref. 31 is that the divergence of S_Q is only logarithmic in 1D; thus S_Q^{-1} does not extrapolate to zero at zero temperature. As shown in Fig. 3(c), coupled $n = 3$ ladders behave completely differently from the isolated $n = 3$ ladder; namely, the S_Q of coupled ladders exhibits a clear crossover from the weak divergence in T^{-1} of an isolated ladder to the strong divergence in T^{-1} of a 2D spin system.

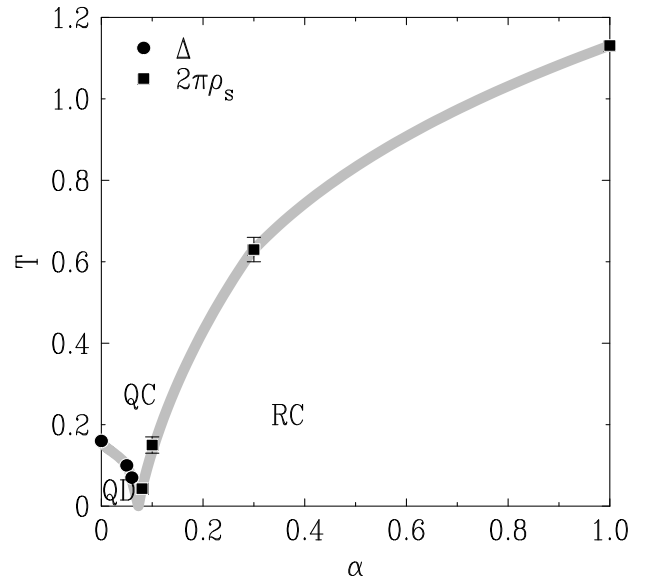


FIG. 4. Phase diagram for weakly coupled four leg ladders. The quantum critical point corresponds to $\alpha = 0.07(1)$, as shown in Fig. 7. The shaded line represents a crossover region rather than a true phase boundary.

IV. WEAKLY COUPLED FOUR LEG LADDERS

Results for $n = 4$, corresponding to Fig. 1(b), are presented in this section. Unlike the $n = 3$ case, an isolated four-leg ladder has a Haldane gap ($\Delta \approx 0.16J$). Therefore, if $\alpha J \ll \Delta$, the ground state remains disordered, and there must then be a quantum phase transition as a function of α at zero temperature at a critical value α_c to

an ordered ground state. In QNL σ M language, there is a quantum critical point dividing the QD ground state and the RC ground state at α_c . We show the phase diagram of arrays of $n = 4$ ladders in Fig. 4. In this figure, we take $2\pi\rho_s$ as the temperature scale where crossover from the QC to the RC regime occurs, and Δ as the crossover temperature from the QC to the QD regime. $2\pi\rho_s$ is determined in the manner explained in Sec. III; Δ can be obtained by fitting to $\chi_u(T) \sim \exp(-\Delta/T)$ at low temperatures ($T \lesssim \Delta$). One should note that the thick shaded lines in Fig. 4 represent crossover lines rather than true phase boundaries. The phase diagram shown here is basically that of the QNL σ M,²¹ with α playing the role of the coupling constant g . As shown in Fig. 4, a quantum critical point occurs at $\alpha_c = 0.07(1)$.

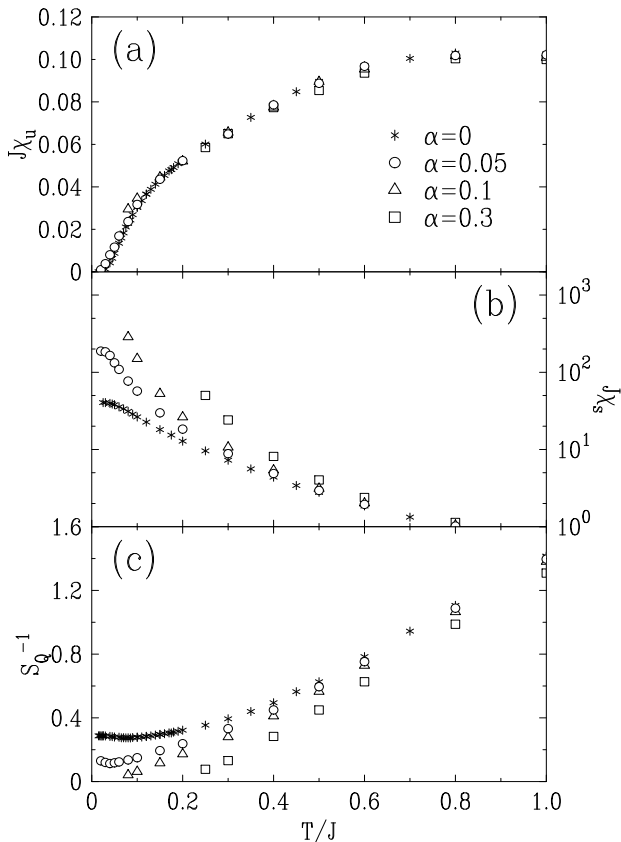


FIG. 5. Uniform susceptibility, staggered susceptibility, and inverse static structure factor peak intensity for arrays of $n = 4$ ladders with different inter-ladder couplings α .

Monte Carlo results for χ_u , χ_s , and S_Q^{-1} are plotted as a function of T , for different α 's, in Fig. 5. The correlation length obtained from the simulation is plotted in Fig. 6 as a function of T^{-1} . Figures 5 and 6 are plotted in such a way as to contrast their behaviors with those of arrays of $n = 3$ ladders. The difference between the behaviors in the QD and the RC regime is evident in these figures; namely, ξ , χ_s , and S_Q all diverge exponentially at low temperatures in the RC regime (e.g., $\alpha = 0.3$), while they all saturate at finite values as $T \rightarrow 0$ in the

QD regime (e.g., $\alpha = 0.05$).

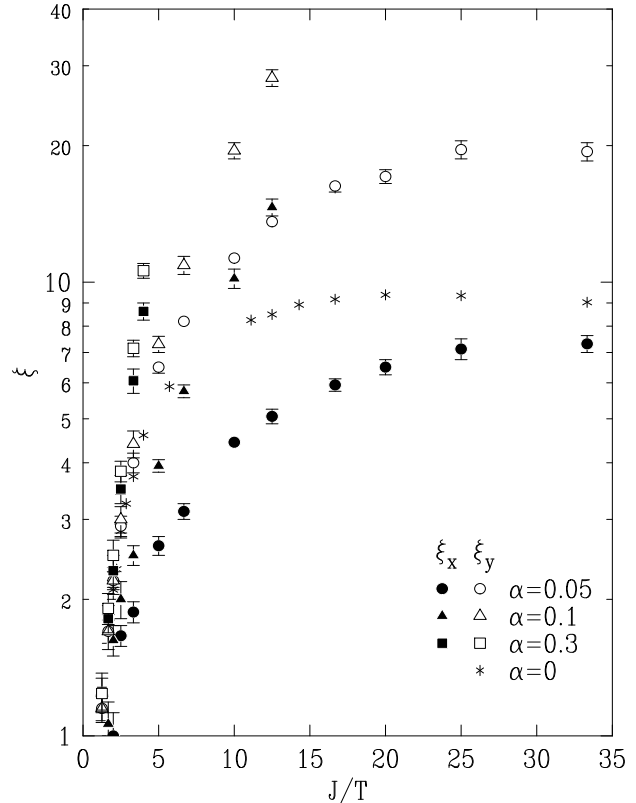


FIG. 6. Correlation lengths for arrays of $n = 4$ ladders with different inter-ladder couplings α plotted as a function of inverse temperature. Correlation lengths in the x -direction are shown as solid symbols, while those in the y -direction are shown as empty symbols.

To illustrate the quantum critical behavior more dramatically, we plot in Fig. 7(a), the dimensionless ratio $S_Q/T\chi_s$. At very high temperatures, this ratio shows classical behavior, $S_Q/T\chi_s = 1$, while the same behavior shows up again at very low temperatures for $\alpha > \alpha_c$, that is, in the RC regime. This is as expected, since RC behavior is closely similar to classical behavior, if the spin wave velocity and spin stiffness renormalizations are accounted for. In the QD regime, that is, $\alpha < \alpha_c$, S_Q and χ_s are constant; therefore $S_Q/T\chi_s$ should be linear in T^{-1} . According to the quantum critical scaling predicted for the QNL σ M,^{34,35} this ratio should show universal behavior in the QC regime with the specific value: $S_Q/T\chi_s = 1.10(2)$. As may be seen in Fig. 7(b), the $\alpha = 0.07$ data for $S_Q/T\chi_s$ indeed are constant $\simeq 1.12$ at low temperatures, in quantitative agreement with the QC theory. This strongly supports the above claim that $\alpha_c = 0.07$ for the $n = 4$ stripe array system is a quantum critical point. Another quantity plotted in Fig. 7(b) is $\xi_y T$. Although $\xi_x T$ is not shown here, it shows essentially the same temperature dependence. Again at very high temperatures, this quantity shows classical behavior, $\xi_y T = J$, while the low-temperature behavior can

distinguish the QC regime from the RC and QD regimes. In the QC regime, the QNL σ M³⁴ predicts $\xi T = c/1.04$, where c is the spin wave velocity. As may be seen in Fig. 7(b), $\xi_y T$ is indeed a constant at low temperatures (high $1/T$) for $\alpha = 0.07$; the explicit value $\xi_y T \simeq 1.4J$ corresponds to $c_y \simeq 1.46J$, close to, but somewhat less than, the value $c = 1.657J$ for the square lattice.³⁶

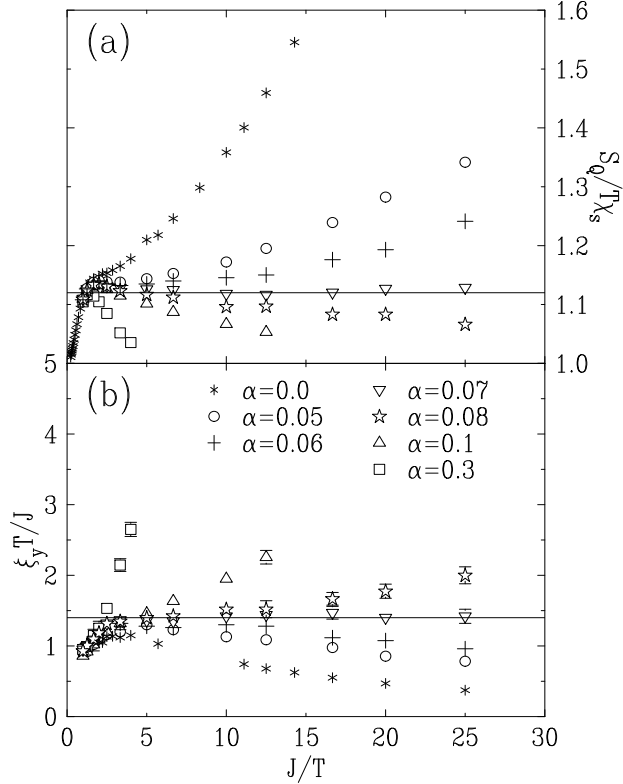


FIG. 7. (a) The ratio $S_Q/T\chi_s$ as a function of inverse temperature as described in the text. (b) The correlation length in the y -direction of arrays of $n = 4$ ladders multiplied by temperature is plotted to contrast the different low-temperature behaviors in the QD and RC phases. The solid lines in both (a) and (b) are the predictions for quantum critical scaling.

V. RANDOM MIXTURE OF WEAKLY COUPLED TWO AND THREE LEG LADDERS

In Fig. 8(a), we show representative static structure factor data at low temperatures for random mixtures of $n = 2$ and $n = 3$ weakly coupled ladders, obtained as described in Sec. II. Here, p is the fraction of $n = 3$ ladders in the mixture; therefore, $p = 1.0$ corresponds to the pure $n = 3$ case. We choose $\alpha = 0.05$ for all of the simulations discussed in this section. We show data at low temperatures ($T \sim 0.05J$), since the magnetic structure factor develops well defined peaks only at these low temperatures. At high temperatures, due to the short correlation lengths, the structure factor exhibits only broad peaks, making it difficult to extract meaningful values for the incommensurability. Nevertheless, we can fit the data with

two identical Lorentzians, split symmetrically about the antiferromagnetic wave vector $\mathbf{Q} \equiv (\pi, \pi)$, together with a broad temperature-independent background term centered around (π, π) :

$$S(q_x, \pi) = \frac{S_Q}{4} \left(\frac{1}{1 + q_+^2/\kappa_x^2} + \frac{1}{1 + q_-^2/\kappa_x^2} \right) + \frac{B}{1 + (q_x - \pi)^2/\kappa_b^2}. \quad (4)$$

Here $q_{\pm} = q_x - (\pi \pm \epsilon)$ and the last term is a temperature-independent background. The width of this background term corresponds to ~ 1 lattice constant. There are only two temperature dependent fitting parameters, ϵ and κ_x , since the peak intensity $S_Q/4$ is calculated separately in our QMC study. The peak position corresponds to the incommensurability ϵ , and the peak width corresponds to the inverse correlation length κ_x . These data are presented in Fig. 9. In Fig. 9(b), we also show $\kappa_y = 1/\xi_y$; ξ_y is computed directly in the way explained in Sec. II.

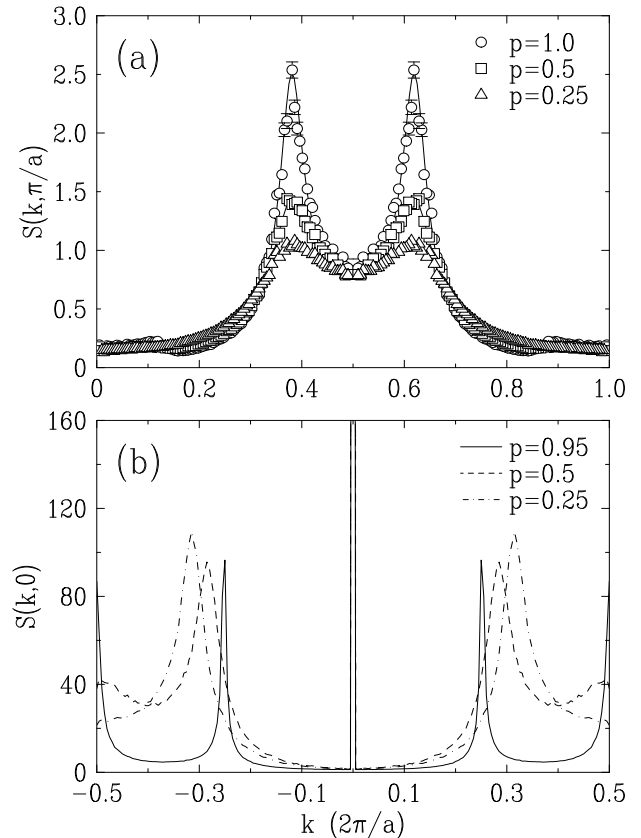


FIG. 8. (a) Static Structure factor near the antiferromagnetic wave vector for the $n = 2$ and $n = 3$ mixed spin ladders. Representative data at $T = 0.05$ for $p = 0.5$ and $p = 0.25$, and at $T = 0.08$ for $p = 1.0$ are shown; $\alpha = 0.05$ for all data. The solid lines are the results of fits to two Lorentzians [Eq. (4)]. (b) Corresponding charge structure factor near the nuclear zone center, calculated as described in the text. We show $p = 0.95$ data instead of $p = 1.0$ for graphical purpose.

The most prominent feature in Fig. 8(a) is that the incommensurability ϵ of the magnetic structure factor does not change significantly as p is varied. This is verified quantitatively in Fig. 9(a), where it may be seen that the values for ϵ for both $p = 0.5$ and $p = 0.25$ cluster around $1/8$, the exact value for $p = 1.0$. Note that the high-temperature data have large error bars, since the peaks are very broad. This behavior of the magnetic structure factor may be contrasted with that of the charge structure factor. We show in Fig. 8(b) the charge structure factor for the charge stripes in the random mixtures. The calculation is made for the simplest charge distribution: we assume that the scattering is unity from the charge stripes (anti-phase domain walls) and zero from the spin ladders. Although greatly oversimplified, as an illustration this calculation nevertheless provides useful intuitive guidance. The most important qualitative result is that the incommensurability of the charge stripes is not equal to twice the magnetic incommensurability in the random mixtures. For example, the $p = 0.25$ case has a charge incommensurability of 0.31 , which is quite different from $2\epsilon = 0.25(2)$, where ϵ is the magnetic incommensurability.

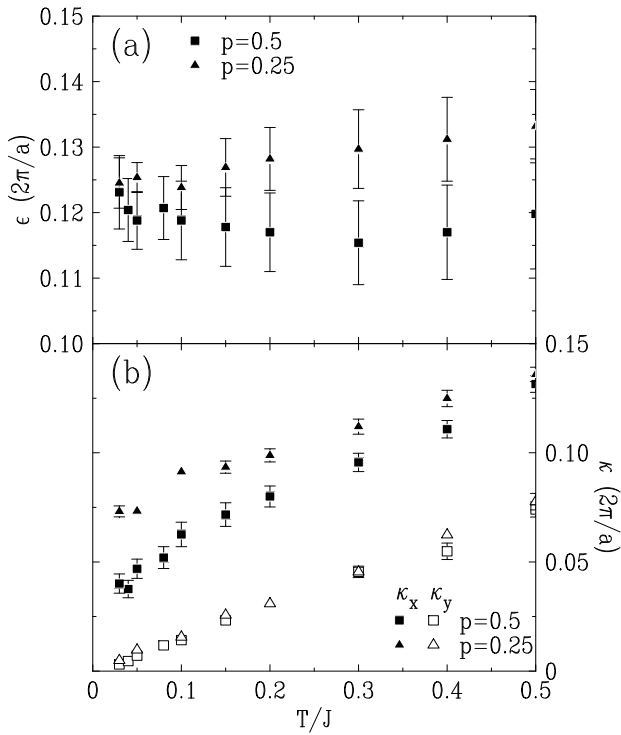


FIG. 9. (a) The incommensurability obtained from the fitting static structure factor to two Lorentzians together with a fixed background term [Eq. (4)]. Even if there is a substantial fraction of $n = 2$ ladders, the incommensurability remains fixed near $1/8$. (b) Inverse correlation length as a function of T . κ_x is obtained from the fit. κ_y is determined from the correlation function Eq. (2b) as described in Sec. II.

This saturation of ϵ of the magnetic structure factor

around $1/8$ can be understood in the following way: At low temperatures ($T \ll \Delta$, $\Delta \approx 0.41J$) the spins on the two-leg ladder will form a spin singlet ground state with a large spin gap in the excitation spectrum. These spin singlets have effective spin zero, and therefore do not contribute in first order to the magnetic structure. Therefore, the magnetic structure factor originates predominantly from the $n = 3$ components of the mixture. In their systematic study of the *dynamic* incommensurate spin fluctuations in $\text{La}_{2-x}\text{Sr}_x\text{CuO}_4$, Yamada and coworkers³ showed that the incommensurability is linear in hole concentration x with $\epsilon \simeq x$ for $0.06 \lesssim x \lesssim 0.12$ and saturates around $1/8$ on further doping. In our simplified model of stripes, the range $0.12 \lesssim x \lesssim 0.16$ corresponds to mixtures of $n = 2$ and $n = 3$ ladders. Although we have calculated the *static* structure factor, we believe that the saturation in the dynamic fluctuation incommensurability in $\text{La}_{2-x}\text{Sr}_x\text{CuO}_4$ may have the same origin. We also have computed χ_u , χ_s , and S_Q^{-1} , which are plotted in Fig. 10 as functions of T , for different p 's, all with $\alpha = 0.05$. Note the differing low-temperature behaviors of the $p = 0$ arrays from those with $p \neq 0$; it is evident that the $n = 3$ physics indeed dominates in the magnetism of the random mixture.

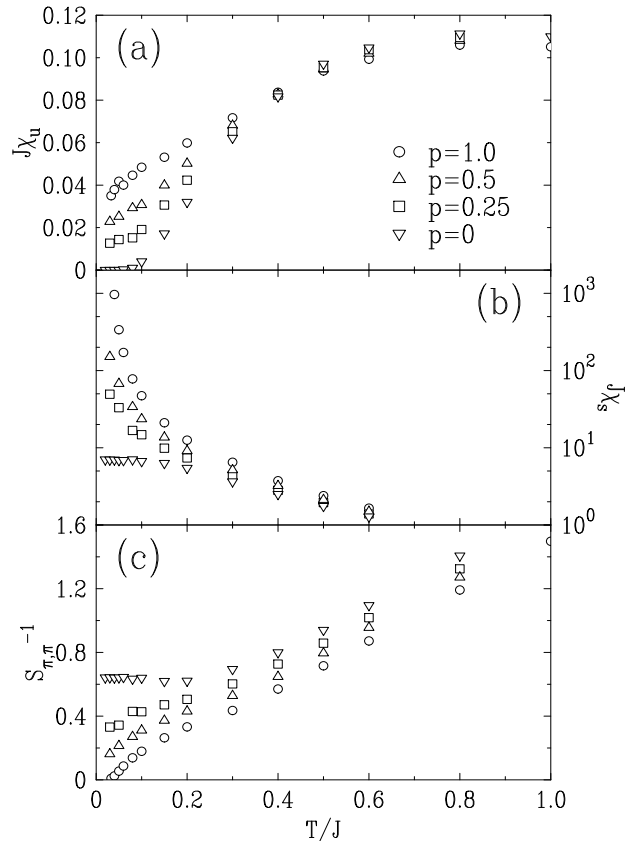


FIG. 10. Uniform susceptibility, staggered susceptibility, and inverse static structure factor peak intensity for arrays of $n = 2$ and $n = 3$ mixed ladders with different p .

Finally, we should note that in our model, in order to

explain the fact that the spin incommensurability saturates near $1/8$ even for very high dopings, we must hypothesize that for doping above the optimal value $x \simeq 0.15$, the charge per stripe increases progressively with increasing x above ~ 0.15 . That is, we assume that as the doping increases beyond $x = 0.15$ charge stripes cannot become closer due to the Coulomb repulsion; instead, additional charges go into already existing charge stripes.

VI. STRONGLY COUPLED THREE LEG LADDERS

The previous calculations have all been done in the weak inter-ladder coupling limit; indeed, in order to obtain reasonable magnetic ordering temperatures in our model, the reduced inter-ladder coupling must be of order $\alpha \sim 0.05$. However, as pointed out to us by Kivelson,³⁷ a similar situation also should obtain in the limit of large α . In this case, physically one would imagine the carriers along the charge stripes mediating a large effective antiferromagnetic exchange between the bounding spin chains; these neighboring chains would then form an array of two-leg ladders coupled to single chains [Fig. 1(a)].

Accordingly, we have carried out a limited number of calculations on arrays of $n = 3$ ladders coupled with strong exchange couplings; that is, in the $\alpha > 1$ limit. Specifically, we have repeated our simulations of Sec. III with $\alpha = 4.0$ and $\alpha = 10.0$. The correlation length data so-obtained are shown in Fig. 11(a). To facilitate a comparison, we have also plotted the $\alpha = 0.05$ data from Fig. 2. At low temperatures, one can see the RC behavior clearly, similar to that of the weak coupling data. The solid lines are the results of fits to Eq. (3). It is evident, however, that the uniform susceptibility data for strongly coupled $n = 3$ ladders shown in Fig. 11(b) are quite different from those of weakly coupled ($\alpha = 0.05$) $n = 3$ ladders. In this limit, since J' is the primary coupling, as discussed above, two-leg ladders are effectively formed across the charge stripes; therefore, we should consider this system as a mixture of $S = 1/2$ chains and $n = 2$ ladders rather than as an array of $n = 3$ ladders. Specifically, $S = 1/2$ chains and $n = 2$ ladders alternate in the x -direction. The spin gap of these $n = 2$ ladders is large (of order $0.5J'$) and the contribution from these to χ_u is essentially zero. Thus one might surmise that χ_u would be entirely due to the $S = 1/2$ chains. That this idea is correct may be seen from Fig. 11(b), where we have plotted the uniform susceptibility per spin of the $S = 1/2$ chain from Ref. 31 divided by three. Both the $\alpha = 4.0$ and the $\alpha = 10.0$ data agree with the spin chain results for $T \gtrsim 0.4J$. At low temperatures, the correlations between the chain and the ladder become important and we observe behavior similar to that of mixtures of ladders [Fig. 10(a)].

The correlation length for $\alpha = 4.0$ grows as a function of T^{-1} much faster than that of $\alpha = 0.05$, such that the

prediction for T_m in this case is $T_m \approx 144K$ for $J = 1500K$, which is more than a factor of three larger than the experimental result. In order to obtain reasonable values for T_m in the large α limit, one needs to have α close to 10 as shown in Fig. 11. In such a case, for $\alpha = 10.0$, we obtain $T_m \approx 55K$. Such large values for $J' \approx 1.3eV$ seem to us to be unlikely. For this model ($J' \gg J$) to be relevant one would need to invoke some other mechanism such as extensive structural disorder or effects from charge and spin fluctuations of the charged stripes themselves to reduce T_m down to the observed values of $30K$ to $40K$.

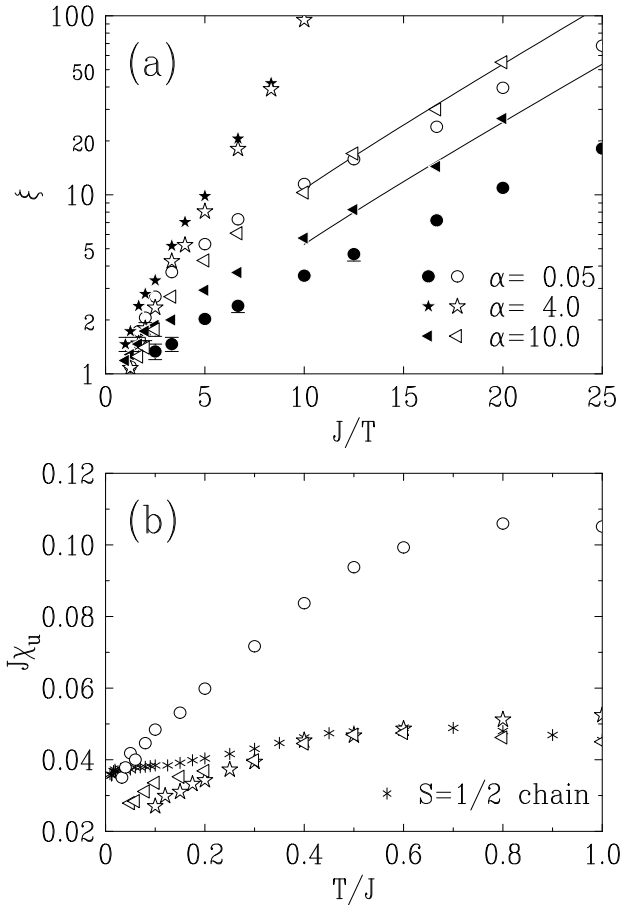


FIG. 11. (a) Correlation lengths for arrays of $n = 3$ ladders with strong inter-ladder coupling ($\alpha > 1$) plotted as a function of inverse temperature. The correlation lengths in the x -direction are shown as solid symbols, while those in the y -direction are shown as empty symbols. (b) Uniform susceptibility per spin as a function of T .

VII. DISCUSSION

A few comments on the applicability of our model are in order. First and foremost, our model is clearly an extremely simplified version of any actual charge and spin ordering in the doped copper oxide planes. We assume that (1) the charge stripes are perfectly ordered

with the charges confined to Cu–O–Cu–O chains and (2) the charge and spin degrees of freedom along the stripes can be ignored. We know that dynamic transverse fluctuations of the charge stripes could be very large, especially for incommensurate charge stripe spacings.¹⁸ However, this effect may be less significant if the charge ordering occurs at a much higher temperature than the spin ordering, so that the charge fluctuations are significantly reduced near the spin ordering temperature. Several neutron scattering experiments on $\text{La}_{2-x}\text{Sr}_x\text{NiO}_4$, and $\text{La}_{1.6-x}\text{Nd}_{0.4}\text{Sr}_x\text{CuO}_4$ indeed report a charge ordering temperature that is higher than the spin ordering temperature.³⁸ The charge degrees of freedom in the metallic stripes, which we have ignored, clearly are essential for the transport and superconducting properties,¹⁸ and we have nothing to contribute on this aspect of the problem. Second, microscopic phase separation of holes and spins can occur in other geometries; for example, it is possible to have *grid-like* spin-rich regions separated by hole-rich domain walls as well as diagonal stripes. In both cases, the incommensurate spin density wave peaks would be rotated by 45° with respect to those for the stripe model discussed here. In a recent experiment on an $x = 0.05$ sample,³⁹ which notably is an insulator rather than a superconductor at low temperatures, 45° rotated magnetic peaks are indeed observed; in that case it is believed that this rotation is due to the establishment of diagonal stripes.

Despite the success of the current model in explaining a number of experimental observations for incommensurabilities near $1/8$, many points remain to be understood. As is obvious in Figs. 2, 5, and 9, ξ_x and ξ_y are very anisotropic, which would, in turn, predict anisotropic widths in the quasielastic and dynamic neutron scattering measurements. Currently available experimental data are not complete enough to test this prediction. In recent work, Tranquada *et al.*¹³ calculated the *elastic* structure factor of $n = 4$ and $n = 3$ mixtures for sinusoidally varying charge and spin density waves; they hypothesized that the stripe disorder is caused by pinning by the random Sr dopants. They also argued that these defects would explain the absence of any peak width anisotropy in their data.

An obvious major deficiency of the current model is that it does not naturally explain the special role which hole dopings x and concomitantly, incommensurabilities ϵ near $1/8$ play in the La_2CuO_4 -based superconductors. It is evident that T_m will be a maximum locally around $x \simeq \epsilon \simeq 1/8$, since for small α , admixtures of $n = 4$ ($x < 1/8$) or $n = 2$ ($x > 1/8$) ladders will decrease the magnetic correlation lengths and hence will lower T_m . However, there is no obvious reason why other odd-width ladder arrays would not also be favorable. We note that for $x < 0.05 = 1/20$ the spin correlations are commensurate¹⁻³ so that the uniform stripe model does not apply. Thus, the other relevant odd-width ladder arrays are $n = 7$, corresponding to $x = \epsilon = 0.0625$, and $n = 5$, corresponding to $x = \epsilon = 0.083$. We have carried

out some limited calculations for $n = 5$ and, as one would intuit from the results of Greven *et al.*¹¹ for isolated ladders, at a given temperature the correlation lengths for arrays of $n = 5$ ladders are somewhat larger than those for $n = 3$ arrays. For perfectly ordered charge stripes, T_m should be correspondingly higher. In fact, the opposite seems to be true, although more experimental data are required to document this completely. At the minimum, from the inelastic neutron scattering studies of Yamada *et al.*,³ we know that the low-energy dynamical coherence length at low temperatures for $x \simeq \epsilon \simeq 1/12$ is shorter than that for $x \simeq \epsilon \simeq 1/8$.

Clearly, therefore, if this stripe model is to describe the real La_2CuO_4 -based superconductors, then some further physics is required. At least three different factors could act to reduce the charge and concomitantly the spin correlation lengths at lower doping. First, as evidenced by the commensurate spin structure for $x \lesssim 0.05$, pinning of the stripes becomes much more important at lower dopings. Second, as the charge stripe separation grows, the stripe-stripe interaction energy will decrease and, correspondingly, stripe positional fluctuations will grow. These would in turn inhibit the development of the spin correlations. Third, as discussed above, it is believed that at $x = 0.05$ the stripes switch from being approximately along the Cu–O–Cu–O direction to being along the diagonal direction,³⁹ that is from $(1\ 0)$ to $(1\ 1)$. Presumably, as the doping decreases towards 0.05 , fluctuations into the diagonal stripe phase could occur and thus would shorten the spin correlation length. These ideas are, of course, purely heuristic. Some real theoretical calculations plus further experiments are clearly required to put the model on a firmer basis.

We have assumed that the charge stripes are site-centered rather than bond-centered.⁴⁰ The basic reason for this is that, at least within our simplified model, we are unable to match at all the observed experimental trends with a bond-centered model. This may be easily seen as follows. First, if the spins across the charged stripe bonds are coupled antiferromagnetically, then the basic commensurate antiferromagnetic situation is unaltered. Second, if, as originally argued by Aharony *et al.*,⁴¹ holes on the oxygens induce a strong ferromagnetic coupling between the two neighboring copper spins, then one has effective $S = 1$ chains. Thus, for the specific case of $\epsilon = 1/8$, the system breaks up into alternating spin-1 chains and two-leg ladders. Both the spin-1 chain ($\Delta \approx 0.4J$) and the two-leg ladder ($\Delta \approx 0.5J$) have large spin gaps and short correlation lengths, so that this system only orders at extremely low temperatures, if at all. On the other hand, for $x = 1/10$ or $x = 1/6$, one has single chains or three-leg ladders respectively in between the spin-1 chains. Hence the correlation length along the chain diverges at low temperature, making a spin density wave ordering possible. The difficulty for a bond-centered model then is that one has facile ordering at $x = 1/10$ and $x = 1/6$, but not at $1/8$, which is the opposite of the general trend observed experimentally. Therefore,

we are required within the context of our model to adopt site-centered stripes in order to obtain sensible behavior around $x = 1/8$ doping regime. It would clearly be interesting to see if this same difficulty occurs for the $t - J$ model as discussed by White and Scalapino.⁴⁰

Manifestly, more experiments are needed to address many unresolved features of the stripe model. First, one needs to understand in detail the doping dependence of the spin density wave ordering in the $\text{La}_{2-x}\text{Sr}_x\text{CuO}_4$ and related systems. Second, better characterization of the charge stripes themselves, including both the incommensurabilities and the correlation lengths is crucial. Third, unambiguous determination of the charge ordering temperatures is essential, since it is still not certain as to whether charge ordering drives the spin ordering, or vice versa.⁴² Since neutrons scatter from the small nuclear displacements induced by the modulated charge density, the charge ordering peaks observed via neutron scattering are extremely weak. Electron diffraction is, of course, especially sensitive to the charge modulation, but it is only useful for surfaces or very thin films which may differ from their bulk counterparts. X-ray scattering seems to be a logical choice to study the charge modulation in these materials. In their study of $\text{La}_{1.48}\text{Nd}_{0.4}\text{Sr}_{0.12}\text{CuO}_4$, Zimmermann *et al.*⁴³ used high-energy x-ray (100 keV) to investigate charge stripes, confirming results from neutron scattering experiments.¹² They were able to determine peak widths at various temperatures with somewhat better precision than that of neutron scattering; however, a much higher resolution x-ray study is necessary to compare quantitatively the correlation length data with various theoretical predictions. Generally, it is important to determine the nature of the charge-charge stripe correlations in both the normal and superconducting states.

In summary, we have studied the magnetism arising from the charge and spin stripe order in monolayer cuprate superconductors. Quantum Monte Carlo simulations have been carried out on a simplified model, which is essentially weakly coupled insulating spin ladders. Our calculations are consistent with recent results of spin density wave ordering and dynamical spin fluctuations in $\text{La}_{2-x}\text{Sr}_x\text{CuO}_4$ and $\text{La}_2\text{CuO}_{4+y}$ for doping and incommensurabilities near $1/8$. We show that the periodicity of the incommensurate spin order is not necessarily twice that of the charge order. The behavior at lower doping remains problematic. We have also studied in detail the quantum critical behavior in coupled four-leg ladders.

ACKNOWLEDGMENTS

We would like to thank V. J. Emery, M. Greven, T. Imai, S. A. Kivelson, and J. M. Tranquada for invaluable discussions. We thank S. A. Kivelson especially for detailed comments on this manuscript. The present work was supported by the US-Japan Cooperative Re-

search Program on Neutron Scattering. The work at Tohoku has been supported by a Grant-in-Aid for Scientific Research of Monbusho and the Core Research for Evolutional Science and Technology (CREST) Project sponsored by the Japan Science and Technology Corporation. The work at MIT was supported by the NSF under Grant No. DMR97-04532 and by the MRSEC Program of the National Science Foundation under Award No. DMR98-08941. The work at Brookhaven National Laboratory was carried out under Contract No. DE-AC02-98CH10886, Division of Materials Science, U. S. Department of Energy.

-
- ¹ Y. Endoh, K. Yamada, M. Matsuda, K. Nakajima, K. Kuroda, Y. Hidaka, I. Tanaka, H. Kojima, R. J. Birgeneau, M. A. Kastner, B. Keimer, G. Shirane, and T. R. Thurston, in *Mechanisms of superconductivity: JJAP series, 7*, edited by Y. Muto (Publication Office, Japanese Journal of Applied Physics, Tokyo, Japan, 1992), pp. 174-177.
 - ² For a review, see M. A. Kastner, R. J. Birgeneau, G. Shirane, and Y. Endoh, *Rev. Mod. Phys.* **70**, 897 (1998).
 - ³ K. Yamada, C. H. Lee, K. Kurahashi, J. Wada, S. Wakimoto, S. Ueki, H. Kimura, Y. Endoh, S. Hosoya, G. Shirane, R. J. Birgeneau, M. Greven, M. A. Kastner, and Y. J. Kim, *Phys. Rev. B* **57**, 6165 (1998).
 - ⁴ N. Bulut, D. Hone, D. J. Scalapino, and N. E. Bickers, *Phys. Rev. Lett.* **64**, 2723 (1990).
 - ⁵ Q. Si, Y. Zha, , K. Levin, and J. P. Lu, *Phys. Rev. B* **47**, 9055 (1993).
 - ⁶ T. Tanamoto, H. Kohno, and H. Fukuyama, *J. Phys. Soc. Jpn* **63**, 2739 (1994).
 - ⁷ J. Zaanen and O. Gunnarsson, *Phys. Rev. B* **40**, 7391 (1989); J. Zaanen, M. L. Horbach, and W. van Saarloos, *ibid.* **53**, 8671 (1996).
 - ⁸ V. J. Emery and S. A. Kivelson, *Physica C* **66**, 763 (1994); S. A. Kivelson and V. J. Emery, in *Strongly Correlated Electronic Materials*, edited by K. S. Bedell, Z. Wang, D. E. Meltzer, A. V. Balatsky, and E. Abrahams (Addison-Wesley, Reading, Massachusetts, 1994), pp. 619-656; V. J. Emery, S. A. Kivelson, and O. Zachar, *Phys. Rev. B* **56**, 6120 (1997).
 - ⁹ C. Nayak and F. Wilczek, *Phys. Rev. Lett.* **78**, 2465 (1997).
 - ¹⁰ For a review, see E. Dagotto and T. M. Rice, *Science* **271**, 618 (1996).
 - ¹¹ M. Greven, R. J. Birgeneau, and U.-J. Wiese, *Phys. Rev. Lett.* **77**, 1865 (1996).
 - ¹² J. M. Tranquada, B. J. Sternlieb, J. D. Axe, Y. Nakamura, and S. Uchida, *Nature* **375**, 561 (1995); J. M. Tranquada, J. D. Axe, N. Ichikawa, Y. Nakamura, S. Uchida, and B. Nachumi, *Phys. Rev. B* **54**, 7489 (1996); J. M. Tranquada, J. D. Axe, N. Ichikawa, A. R. Moodenbaugh, Y. Nakamura, and S. Uchida, *Phys. Rev. Lett.* **78**, 338 (1997).
 - ¹³ J. M. Tranquada, N. Ichikawa, and S. Uchida,

- cond-mat/9810212.
- ¹⁴ T. Suzuki, T. Goto, K. Chiba, T. Shinoda, T. Fukase, H. Kimura, K. Yamada, M. Ohashi, and Y. Yamaguchi, *Phys. Rev. B* **57**, R3229 (1998).
 - ¹⁵ H. Kimura, K. Hirota, H. Matsushita, K. Yamada, Y. Endoh, S. H. Lee, C. F. Majkrzak, R. Erwin, G. Shirane, M. Greven, Y. S. Lee, M. A. Kastner, and R. J. Birgeneau, *Phys. Rev. B* (to be published).
 - ¹⁶ Y. S. Lee, R. J. Birgeneau, M. A. Kastner, Y. Endoh, S. Wakimoto, K. Yamada, R. W. Erwin, S. H. Lee, and G. Shirane, cond-mat/9902157.
 - ¹⁷ P. Dai, H. A. Mook, and F. Doğan, *Phys. Rev. Lett.* **80**, 1738 (1998); H. A. Mook, P. Dai, S. M. Hayden, G. Aeppli, T. G. Perring, and F. Doğan, *Nature* **395**, 580 (1998).
 - ¹⁸ S. A. Kivelson, E. Fradkin, and V. J. Emery, *Nature* **393**, 550 (1998); S. A. Kivelson and V. J. Emery, cond-mat/9809082.
 - ¹⁹ C. Nayak and F. Wilczek, *Int. J. Mod. Phys. B* **10**, 2125 (1996).
 - ²⁰ C. Kim, P. J. White, Z.-X. Shen, T. Tohyama, Y. Shibata, S. Maekawa, B. O. Wells, Y. J. Kim, R. J. Birgeneau, and M. A. Kastner, *Phys. Rev. Lett.* **80**, 4245 (1998).
 - ²¹ S. Chakravarty, B. I. Halperin, and D. R. Nelson, *Phys. Rev. Lett.* **60**, 1057 (1988); S. Chakravarty, B. I. Halperin, and D. R. Nelson, *Phys. Rev. B* **39**, 2344 (1989).
 - ²² P. Hasenfratz and F. Niedermayer, *Phys. Lett. B* **268**, 231 (1991).
 - ²³ M. Greven, R. J. Birgeneau, Y. Endoh, M. A. Kastner, M. Matsuda, and G. Shirane, *Z. Phys. B* **96**, 465 (1995).
 - ²⁴ R. J. Birgeneau, A. Aharony, N. R. Belk, F. C. Chou, Y. Endoh, M. Greven, S. Hosoya, M. A. Kastner, C. H. Lee, Y. Lee, G. Shirane, S. Wakimoto, B. O. Wells, and K. Yamada, *J. Phys. Chem. Solids* **56**, 1913 (1995).
 - ²⁵ For a review, see I. Affleck, *J. Phys. Condens. Matter* **1**, 3047 (1989).
 - ²⁶ F. D. M. Haldane, *Phys. Lett.* **93A**, 464 (1983).
 - ²⁷ M. Nightingale and H. Blöte, *Phys. Rev. B* **33**, 659 (1986).
 - ²⁸ J. Renard, M. Verdaguer, L. Regnault, W. Erkelens, J. Rossat-Mignod, and W. Stirling, *Europhys. Lett.* **3**, 945 (1987).
 - ²⁹ J. Tworzydło, O. Y. Osman, C. N. A. van Duin, and J. Zaanen, *Phys. Rev. B* **59**, 115 (1999).
 - ³⁰ For a review, see H. G. Evertz, in *Numerical Methods for Lattice Many-Body Problems*, edited by D. J. Scalapino (Addison Wesley Longman, Reading, Massachusetts, 1998), p. 6.
 - ³¹ Y. J. Kim, M. Greven, U.-J. Wiese, and R. J. Birgeneau, *Eur. Phys. J. B* **4**, 291 (1998).
 - ³² A. H. Castro Neto and D. Hone, *Phys. Rev. Lett.* **76**, 2165 (1996).
 - ³³ B. Keimer, N. Belk, R. J. Birgeneau, A. Cassanho, C. Y. Chen, M. A. Kastner, A. Aharony, Y. Endoh, R. W. Erwin, and G. Shirane, *Phys. Rev. B* **46**, 14034 (1992).
 - ³⁴ A. V. Chubukov, S. Sachdev, and A. Sokol, *Phys. Rev. B* **49**, 9052 (1994); A. V. Chubukov, S. Sachdev, and J. Ye, *ibid.* **49**, 11919 (1994).
 - ³⁵ A. Sokol, R. L. Glenister, and R. R. P. Singh, *Phys. Rev. Lett.* **72**, 1549 (1994).
 - ³⁶ B. B. Beard, R. J. Birgeneau, M. Greven, and U. J. Wiese, *Phys. Rev. Lett.* **80**, 1742 (1998).
 - ³⁷ S. A. Kivelson (private communication).
 - ³⁸ For a review, see J. M. Tranquada, in *Neutron Scattering in Layered Copper-Oxide Superconductors*, edited by A. Furrier (Kluwer, Dordrecht, The Netherlands, 1998), pp. 225-260.
 - ³⁹ S. Wakimoto, R. J. Birgeneau, Y. Endoh, P. M. Gehring, K. Hirota, M. A. Kastner, S. H. Lee, Y. S. Lee, G. Shirane, S. Ueki, and K. Yamada, cond-mat/9902201.
 - ⁴⁰ S. R. White and D. J. Scalapino, *Phys. Rev. Lett.* **80**, 1272 (1998).
 - ⁴¹ A. Aharony, R. J. Birgeneau, A. Coniglio, M. A. Kastner, and H. E. Stanley, *Phys. Rev. Lett.* **60**, 1330 (1988).
 - ⁴² O. Zachar, S. A. Kivelson, and V. J. Emery, *Phys. Rev. B* **57**, 1422 (1998).
 - ⁴³ M. v. Zimmermann, A. Vigliante, T. Niemöller, N. Ichikawa, T. Frello, J. Madsen, P. Wochner, S. Uchida, N. H. Andersen, J. M. Tranquada, D. Gibbs, and J. R. Schneider, *Europhys. Lett.* **41**, 629 (1998).